

Nonblind Image Deconvolution via Leveraging Model Uncertainty in An Untrained Deep Neural Network (Supplementary Materials)

Mingqin Chen¹, Yuhui Quan^{1*}, Tongyao Pang² and Hui Ji²

¹School of Computer Science and Engineering, South China University of Technology,
Guangzhou, 510006, China.

²Department of Mathematics, National University of Singapore, 119076, Singapore.

*Corresponding author.

Contents

A An Empirical Study on The Relation Between Kernel Accuracy and Performance of The Proposed Method	2
B Results of Ablation Study on Set12	4
C More Visual Results in Limitation Analysis	4
D More Visual Results in The Experiments	5

A An Empirical Study on The Relation Between Kernel Accuracy and Performance of The Proposed Method

Extensive experiments conducted in the main paper showed that the proposed method has overall better robustness to kernel error than existing non-blind deconvolution methods, in the application of blind motion deblurring. The amount of kernel error in these experiments ranges from small to very large. In this experiment, we would like to see at what range of the amount of kernel error, the proposed method performs better than the existing ones.

The experiments are conducted on the Levin *et al.*'s dataset using the estimated kernels sampled from the intermediate results of SelfDeblur (Ren *et al.*, 2020). That is, we sampled the estimated kernels and estimated latent images from SelfDeblur at every 100 iterations. Then, the intermediate deblurred results from SelfDeblur are compared to the one from the proposed methods (note that both use the same intermediate estimation of motion-blur kernel).

The accuracy of kernel estimation is measured by the maximum of normalized convolution cross-correlation (MNC) (Ren *et al.*, 2020). See Fig. 1 for the PSNR and MNC curve. It can be seen that the proposed method can't yield reasonable results in the very early stage (before 400 iterations) where the MNC is lower than 0.71. After 400 iterations, the kernel error decreases to a medium amount, and the proposed method start to perform better than SelfDeblur. The advantage of the proposed method is kept unchanged afterward (around $> 0.3dB$ after convergence). See Fig. 2 for visual results.

This empirical study shows that the proposed method can handle well the small to medium amount of kernel error. The range where the proposed works well is $[0.7, 0.95]$ (in MNC) in the experiment. In other words, a blind deblurring method can call the proposed method for deblurring the image during the iteration to speed up the convergence, as long the estimation of the kernel is not too far way from the truth kernel.

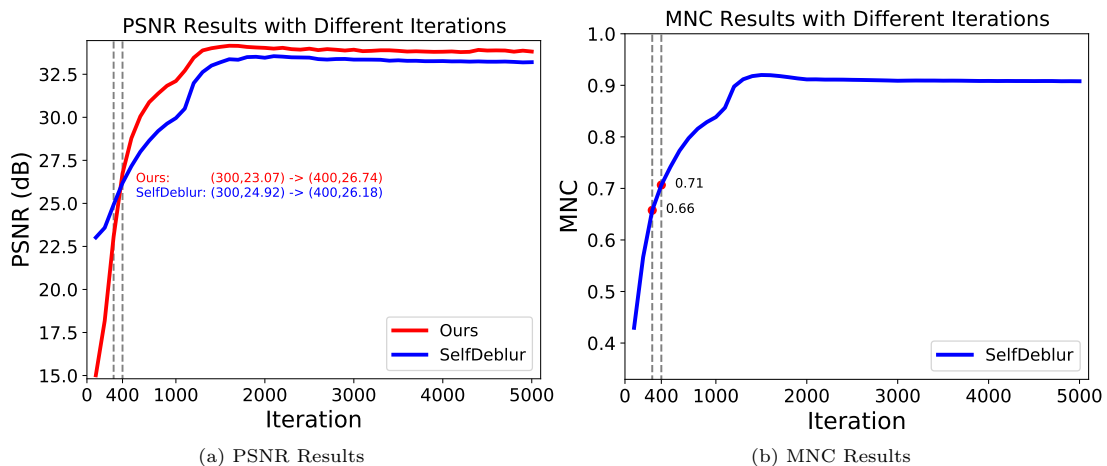


Fig. 1 Quantitative results on Levin *et al.*'s dataset with different intermediate kernels generated from SelfDeblur.

	0.284	0.370	0.394	0.428	0.489	0.549	0.600	GT (MNC)
Kernel								
	18.98dB	18.95dB	20.01dB	21.12dB	22.53dB	24.34dB	25.70dB	Input (PSNR)
SelfDeblur								
	11.81dB	13.75dB	15.85dB	18.52dB	21.98dB	25.44dB	27.31dB	GT (PSNR)
Ours								
	#100	#200	#300	#400	#500	#600	#700	Iteration
	0.632	0.642	0.646	0.724	0.745	0.750	0.752	GT(MNC)
Kernel								
	26.79dB	27.54dB	28.15dB	33.49dB	33.76dB	33.75dB	33.73dB	Input (PSNR)
SelfDeblur								
	28.28dB	29.32dB	29.97dB	33.63dB	33.96dB	34.06dB	34.10dB	GT (PSNR)
Ours								
	#800	#900	#1000	#2000	#3000	#4000	#5000	Iteration

Fig. 2 Visual results of motion deblurring with different intermediate kernels generated from SelfDeblur.

B Results of Ablation Study on Set12

The ablation study is also conducted on Set12 in NID with accurate motion kernels. See following tables for the results.

Table 1 PSNR(dB) results in ablation studies on Set12 with accurate motion kernels and AWGN ($\sigma = 5\%$).

Dropout	Noise Level σ			Peak Value			
	1%	3%	5%	128	256	512	1024
Standard	32.04	28.85	27.62	26.41	27.62	28.57	29.57
SA	32.09	28.97	27.75	26.98	27.90	28.87	29.81
Margin	0.05	0.12	0.13	0.37	0.28	0.30	0.24

Table 2 Quantitative results in ablation studies on Set with accurate motion kernels and AWGN ($\sigma = 5\%$).

w/o	Dropout	Aggregat.	Replace.	Masking	Ours
PSNR(dB)	23.71	24.10	26.12	26.28	26.56
SSIM	0.579	0.588	0.732	0.760	0.770

C More Visual Results in Limitation Analysis

The following figures show that the proposed method does not work well on large kernel error.



Fig. 3 Failure case of the proposed method when deblurring on images from Lai *et al.*'s synthetic dataset in the presence of large kernel error.

D More Visual Results in The Experiments

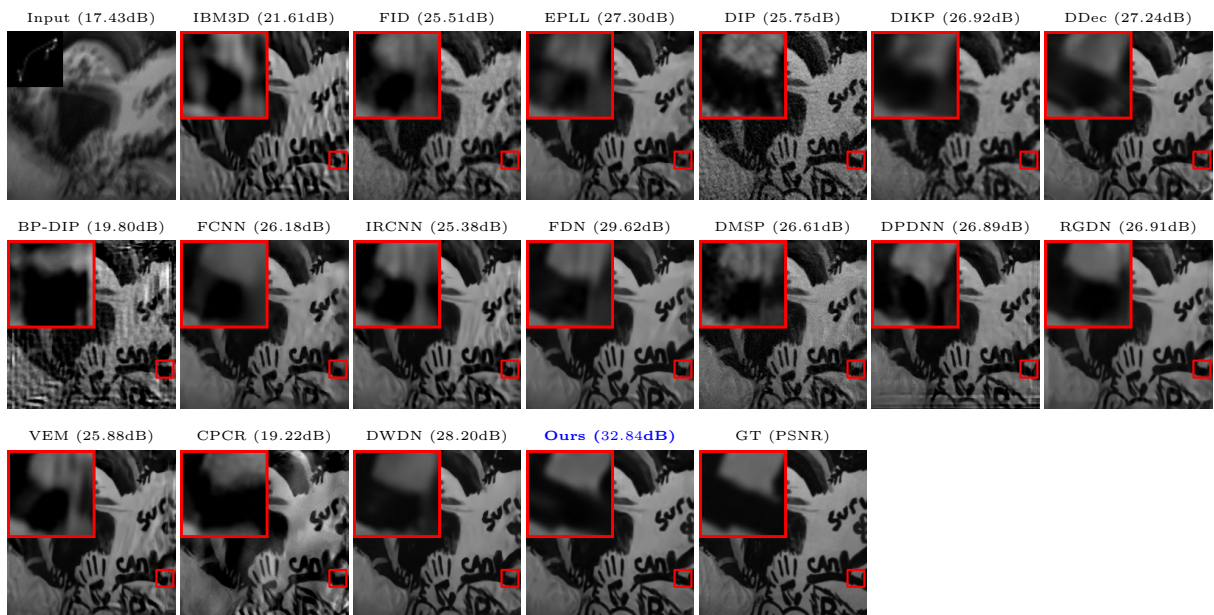


Fig. 4 Visual results of nonblind motion deblurring on a blurry image from Levin *et al.*'s dataset.(4th kernel from (Levin *et al.*, 2011) and noise level $\sigma = 2.55$).

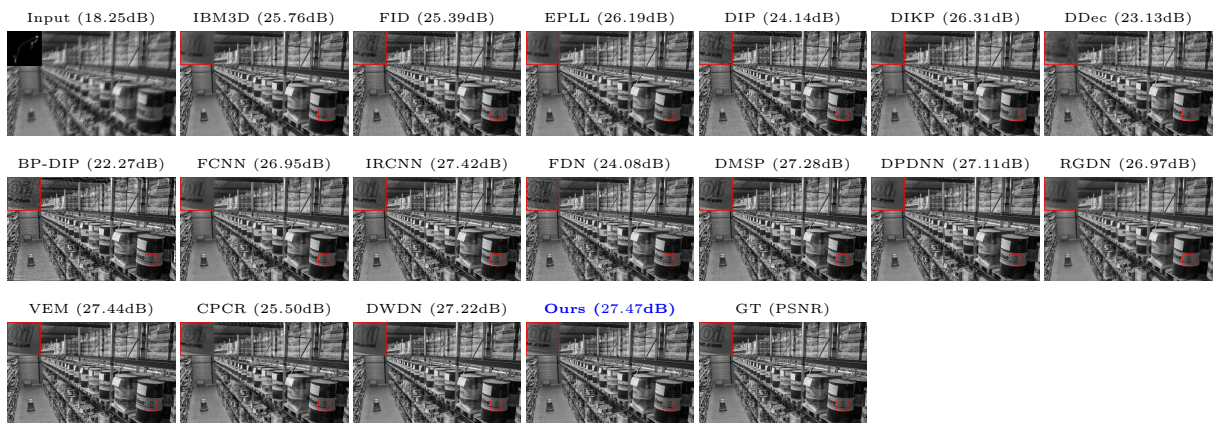


Fig. 5 Visual results of nonblind motion deblurring on a blurry image from Sun *et al.*'s dataset (4th kernel from (Levin *et al.*, 2011) and noise level $\sigma = 7.65$).

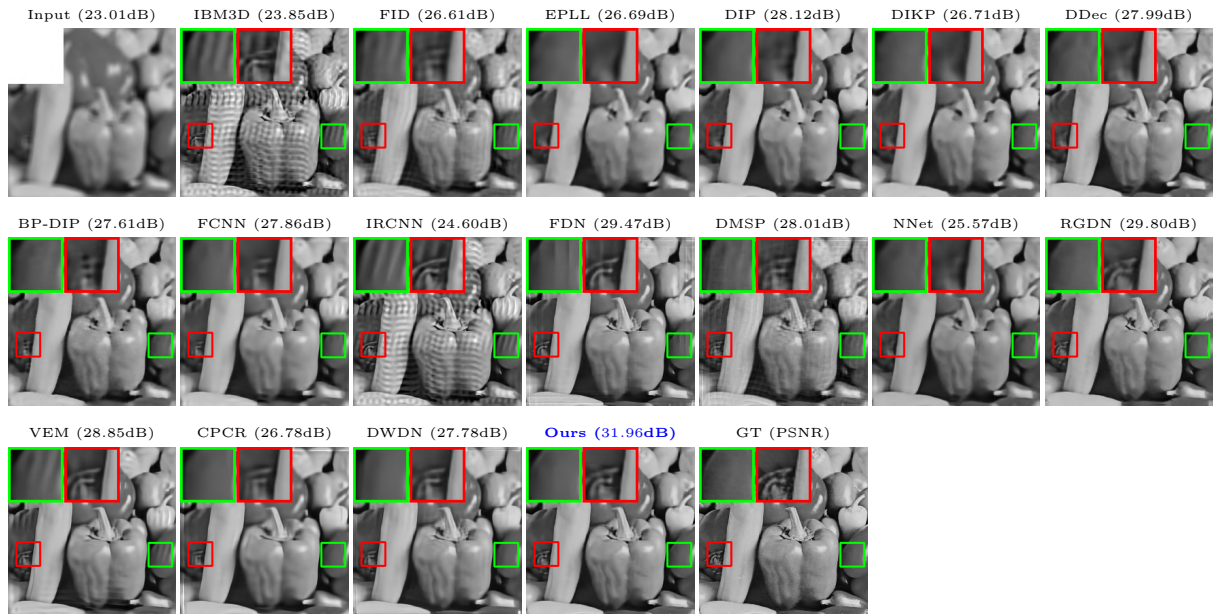


Fig. 6 Visual results of nonblind motion deblurring on a blurry image from Set12 (3rd scenario from (Danielyan et al, 2011)).

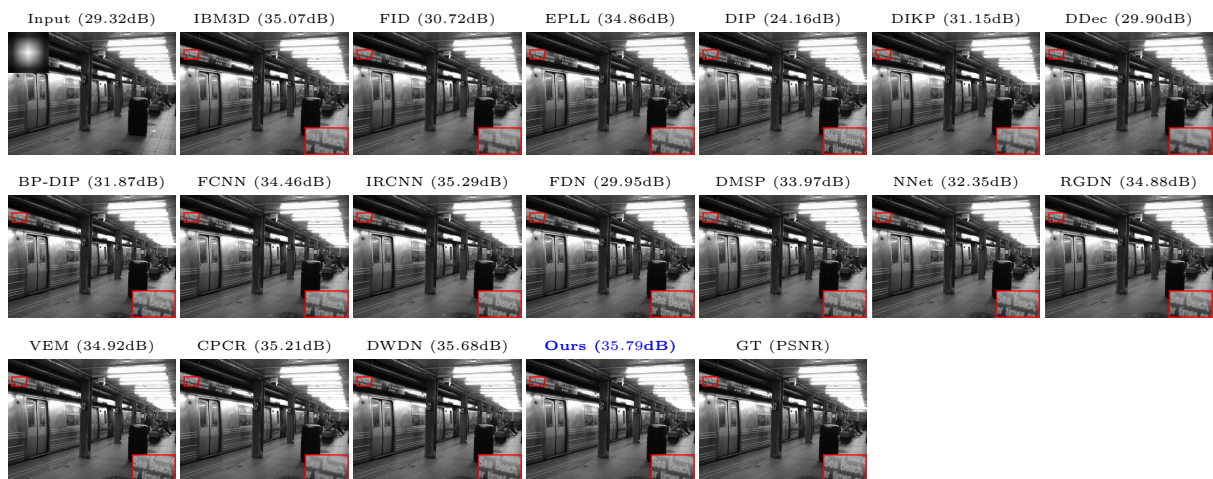


Fig. 7 Visual results of nonblind deblurring on a blurry image from Sun *et al.*'s dataset (4th scenario from (Danielyan et al, 2011)).

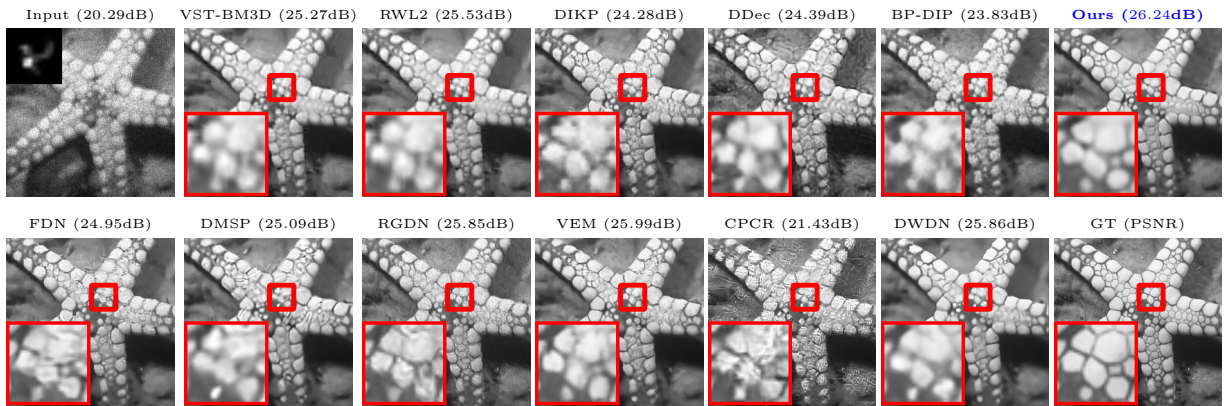


Fig. 8 Visual results of nonblind deblurring on a blurry image with Poisson noise from Set12 (5th kernel from (Levin et al, 2011) and peak = 128).

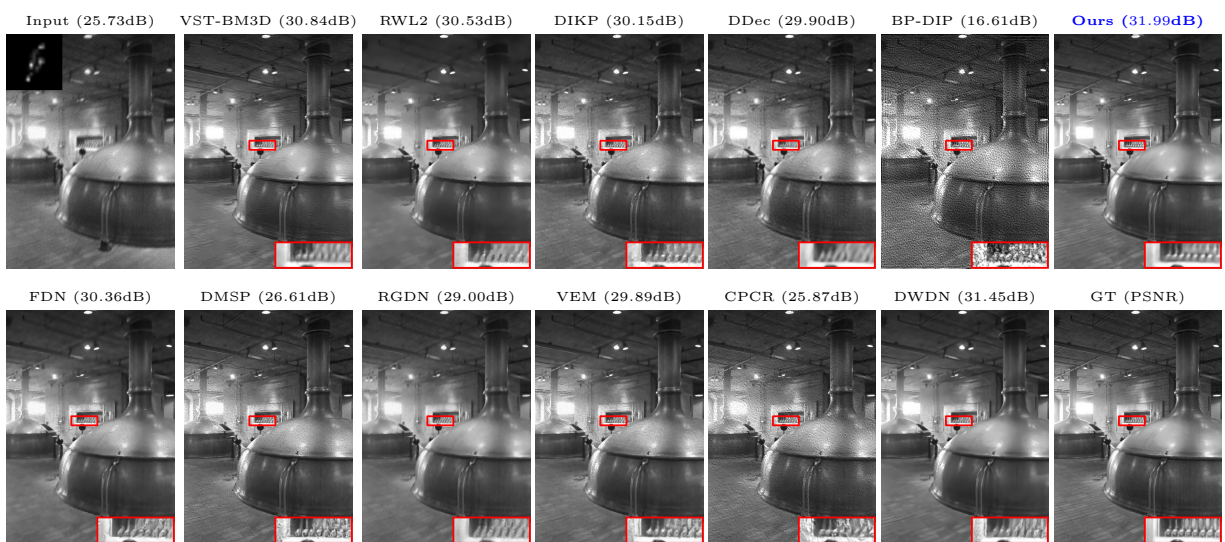


Fig. 9 Visual results of nonblind deblurring on a blurry image with Poisson noise from Sun *et al.*'s dataset (1st kernel from (Levin et al, 2011) and peak = 256).

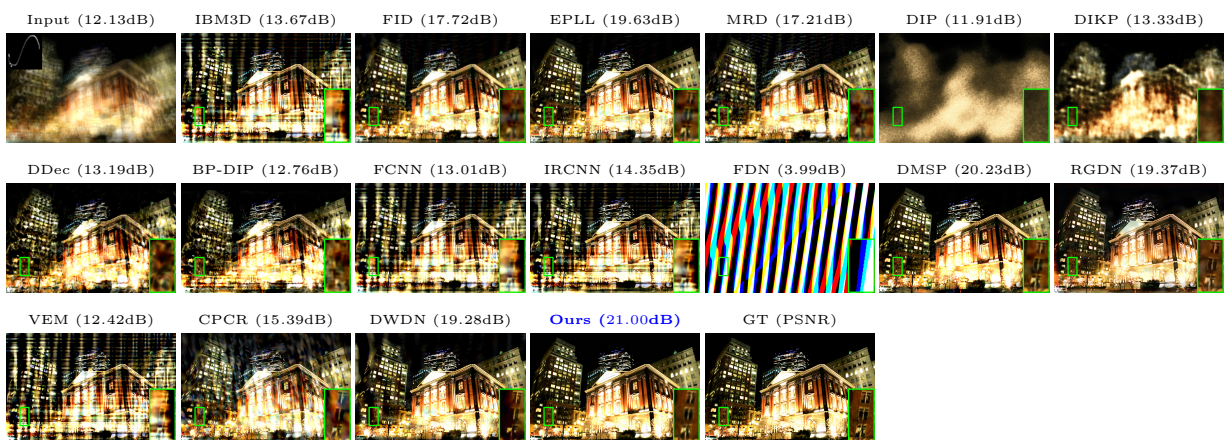


Fig. 10 Visual results of motion deblurring on a blurry image with real-world degradation from Lai *et al.*'s dataset (4th kernel from (Lai et al, 2016) and $\sigma = 2.55$).

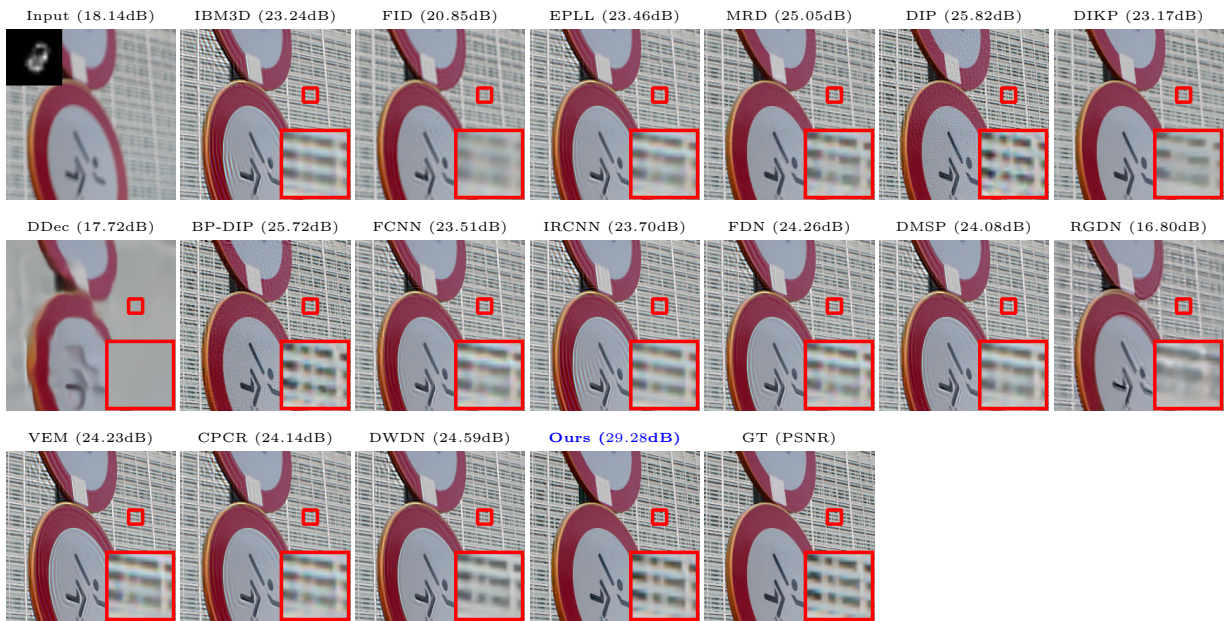


Fig. 11 Visual results of motion deblurring on a blurry image with real-world degradation from Anger *et al.*'s dataset (3th kernel from (Levin *et al*, 2011) and $\sigma = 2.55$).

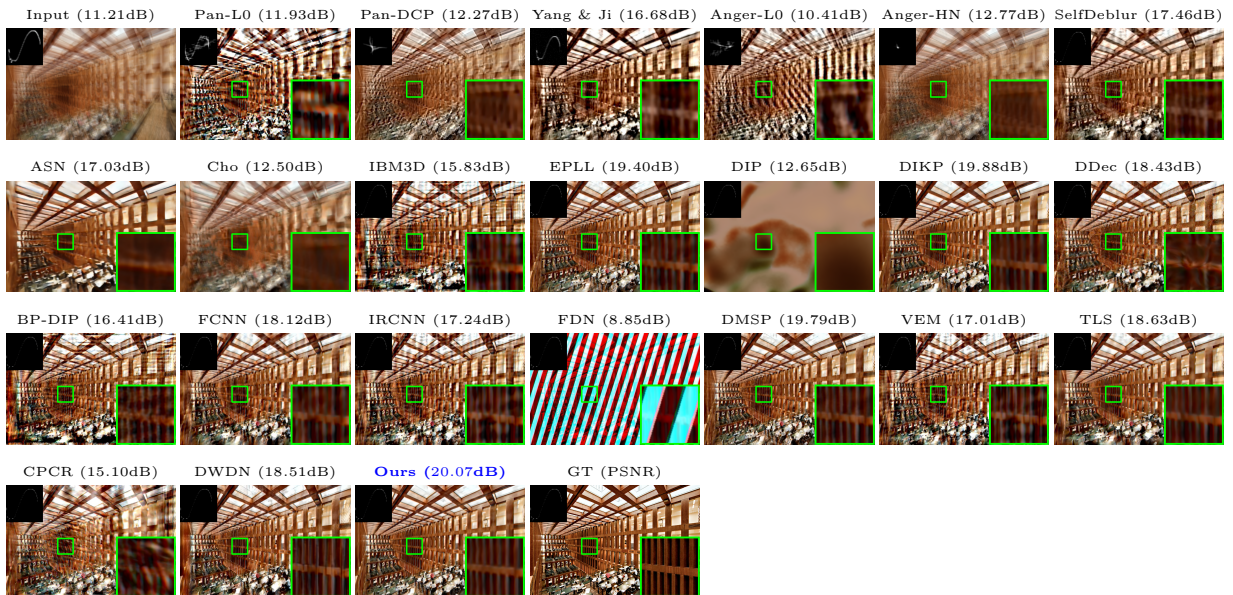


Fig. 12 Visual results of real motion deblurring on a blurry image from Lai *et al.*'s dataset with inaccurate kernels.(4th kernel from (Lai *et al*, 2016)).

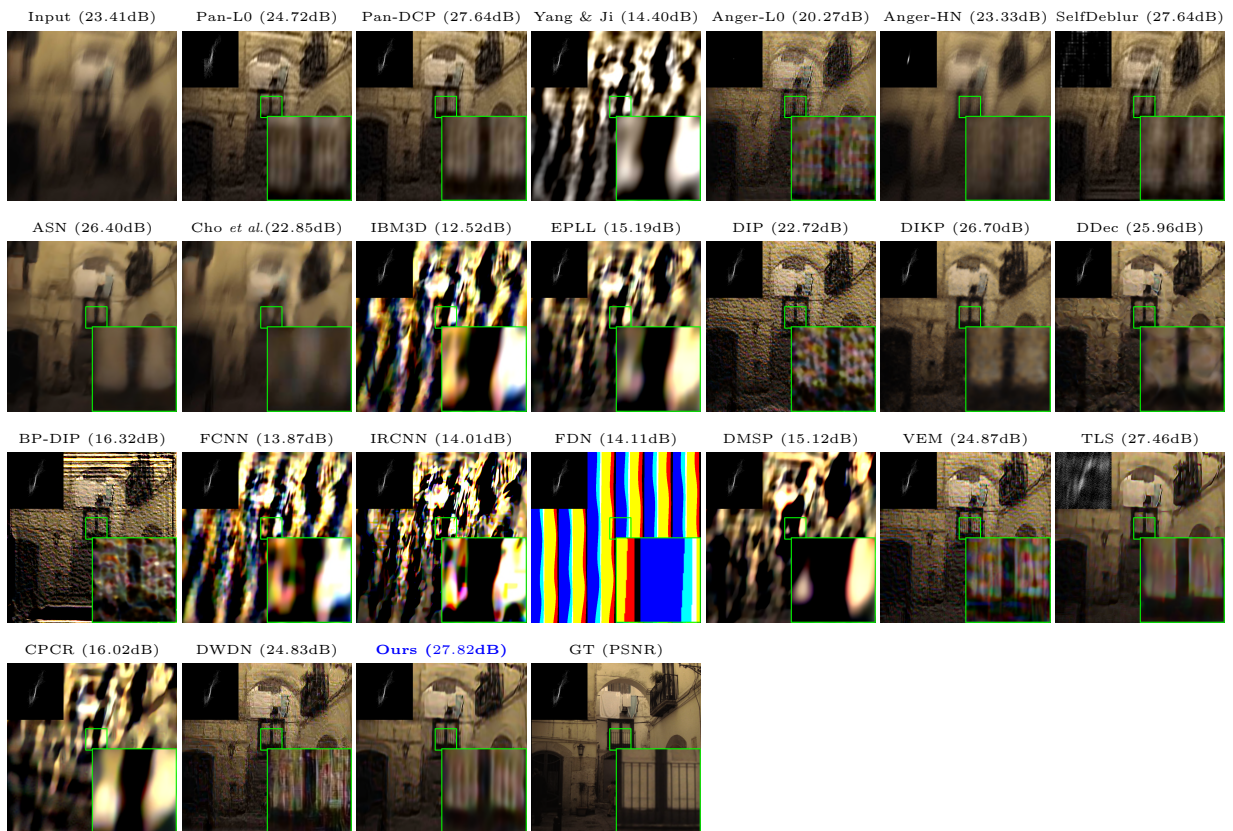


Fig. 13 Visual results of real motion deblurring on a blurry image from Kohler *et al.*'s dataset with inaccurate kernels. (10th kernel from (Köhler *et al.*, 2012)).

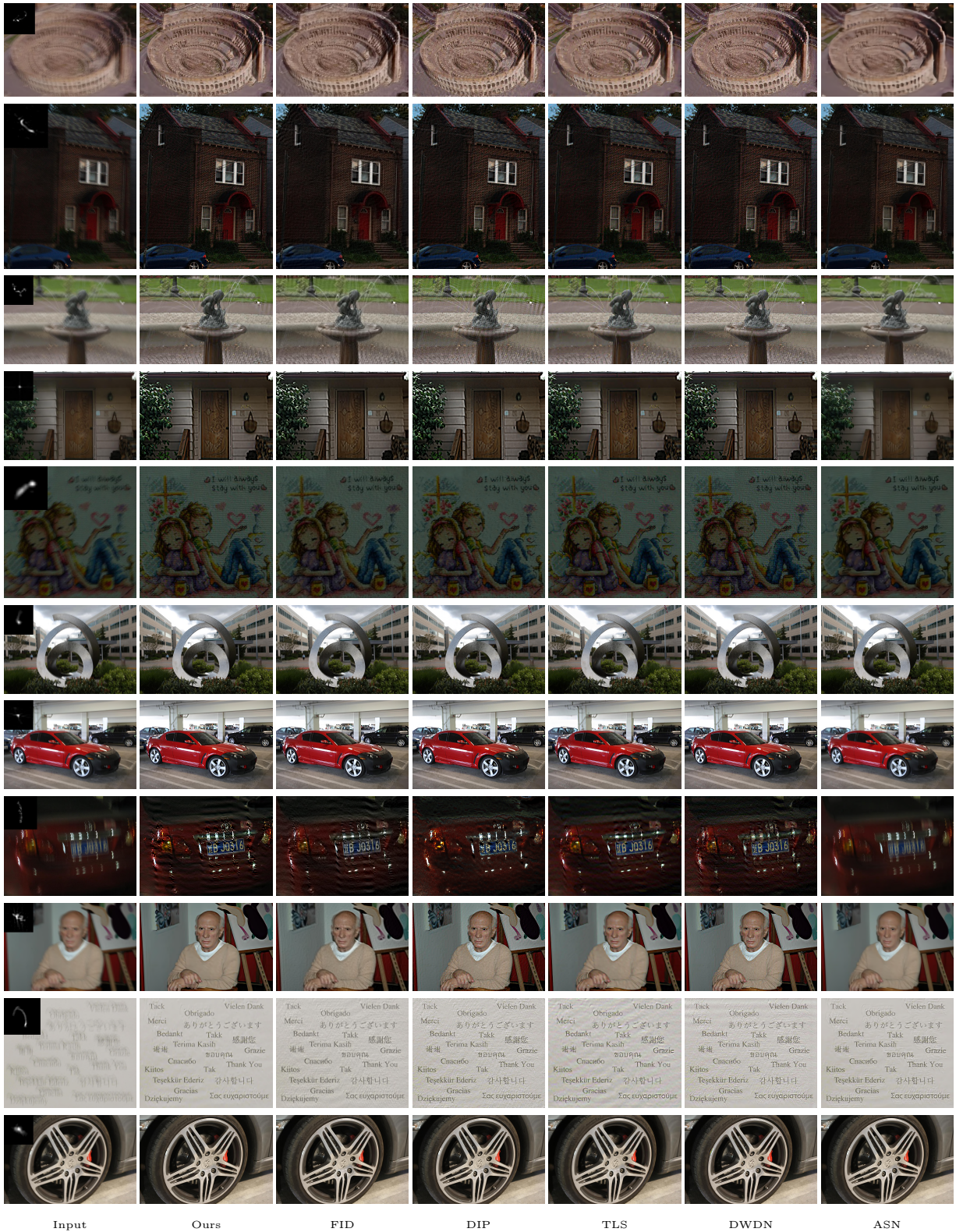


Fig. 14 Visual results of real motion deblurring on Lai *et al.*'s real dataset.

References

- Danielyan A, Katkovnik V, Egiazarian K (2011) Bm3d frames and variational image deblurring. *IEEE Transactions on Image Processing* 21(4):1715–1728
- Köhler R, Hirsch M, Mohler B, Schölkopf B, Harmeling S (2012) Recording and playback of camera shake: Benchmarking blind deconvolution with a real-world database. In: *Proceedings of the European Conference on Computer Vision*, Springer, pp 27–40
- Lai WS, Huang JB, Hu Z, Ahuja N, Yang MH (2016) A comparative study for single image blind deblurring. In: *Proceedings of the IEEE Conference on Computer Vision and Pattern Recognition*, pp 1701–1709
- Levin A, Weiss Y, Durand F, Freeman WT (2011) Efficient marginal likelihood optimization in blind deconvolution. In: *Proceedings of the IEEE Conference on Computer Vision and Pattern Recognition*, IEEE, pp 2657–2664
- Ren D, Zhang K, Wang Q, Hu Q, Zuo W (2020) Neural blind deconvolution using deep priors. In: *Proceedings of the IEEE/CVF Conference on Computer Vision and Pattern Recognition*, pp 3341–3350